

# Signal Transducer and Activator of Transcription-5 Mediates Neuronal Apoptosis Induced by Inhibition of Rac GTPase Activity\*

Received for publication, September 7, 2011, and in revised form, February 13, 2012. Published, JBC Papers in Press, February 29, 2012, DOI 10.1074/jbc.M111.302166

Trisha R. Stankiewicz<sup>†1</sup>, F. Alexandra Loucks<sup>§1</sup>, Emily K. Schroeder<sup>§</sup>, Marja T. Nevalainen<sup>¶</sup>, Kenneth L. Tyler<sup>||</sup>, Klaus Aktories<sup>\*\*</sup>, Ron J. Bouchard<sup>§</sup>, and Daniel A. Linseman<sup>†§‡‡</sup>

From the <sup>†</sup>Department of Biological Sciences and Eleanor Roosevelt Institute, University of Denver, Denver, Colorado 80208,

<sup>§</sup>Research Service, Veterans Affairs Medical Center, Denver, Colorado 80220, <sup>¶</sup>Department of Cancer Biology and Kimmel Cancer Center, Thomas Jefferson University, Philadelphia, Pennsylvania 19107, <sup>||</sup>Department of Neurology and <sup>‡‡</sup>Division of Clinical Pharmacology and Toxicology, Department of Medicine and Neuroscience Program, University of Colorado Denver, Aurora, Colorado 80045, and <sup>\*\*</sup>Institute of Experimental and Clinical Pharmacology and Toxicology, Albert-Ludwigs-Universität Freiburg, D79104 Freiburg, Germany

**Background:** Rac GTPase functions to promote survival in primary cerebellar granule neurons.

**Results:** Rac GTPase inhibition induces STAT5 activation, recruitment of STAT5 to the Bcl-xL promoter, and STAT5-dependent apoptosis.

**Conclusion:** A novel proapoptotic JAK/STAT5 pathway is activated downstream of Rac GTPase inhibition in neurons.

**Significance:** This is the first study to implicate STAT5 as a proapoptotic factor in neurons.

In several neuronal cell types, the small GTPase Rac is essential for survival. We have shown previously that the Rho family GTPase inhibitor *Clostridium difficile* toxin B (ToxB) induces apoptosis in primary rat cerebellar granule neurons (CGNs) principally via inhibition of Rac GTPase function. In the present study, incubation with ToxB activated a proapoptotic Janus kinase (JAK)/signal transducer and activator of transcription (STAT) pathway, and a pan-JAK inhibitor protected CGNs from Rac inhibition. STAT1 expression was induced by ToxB; however, CGNs from STAT1 knock-out mice succumbed to ToxB-induced apoptosis as readily as wild-type CGNs. STAT3 displayed enhanced tyrosine phosphorylation following treatment with ToxB, and a reputed inhibitor of STAT3, curcumin (JSI-124), reduced CGN apoptosis. Unexpectedly, JSI-124 failed to block STAT3 phosphorylation, and CGNs were not protected from ToxB by other known STAT3 inhibitors. In contrast, STAT5A tyrosine phosphorylation induced by ToxB was suppressed by JSI-124. In addition, roscovitine similarly inhibited STAT5A phosphorylation and protected CGNs from ToxB-induced apoptosis. Consistent with these results, adenoviral infection with a dominant negative STAT5 mutant, but not wild-type STAT5, significantly decreased ToxB-induced apoptosis of CGNs. Finally, chromatin immunoprecipitation with a STAT5 antibody revealed increased STAT5 binding to the promoter region of prosurvival Bcl-xL. STAT5 was recruited to the Bcl-xL promoter region in a ToxB-dependent manner, and this DNA binding preceded Bcl-xL down-regulation, suggesting tran-

scriptional repression. These data indicate that a novel JAK/STAT5 proapoptotic pathway significantly contributes to neuronal apoptosis induced by the inhibition of Rac GTPase.

Rho family GTPases are important mediators of cellular development, survival, and death. The most well characterized members of the family are RhoA, Rac1, and Cdc42. Although best known for regulating actin cytoskeletal dynamics, Rho GTPases also play important roles in cell cycle progression (1), gene transcription (2), and cell-cell or cell-matrix adhesion (3, 4). In recent years, the role of Rho GTPases in neuronal survival has begun to be investigated. For example, inhibitors of 3-HMG-CoA reductase (statins) decrease the localization of Rho GTPases to the plasma membrane and induce apoptosis in rat cortical neurons (5). We have shown previously that the function of Rac is essential for the survival of cerebellar granule neurons (CGNs)<sup>3</sup> as the inhibition of Rac with either large clostridial cytotoxins or overexpression of a dominant negative Rac mutant induces mitochondrially dependent apoptosis of these cells (6). In a similar manner, use of either dominant negative Rac or siRNA against the Rac guanine nucleotide exchange factor alsin (ALS2) results in apoptosis of primary cultured spinal motor neurons (7). The critical role of Rac in neuronal survival is further evidenced by the finding that ALS2 is mutated in juvenile onset amyotrophic lateral sclerosis. Although changes in Rac activity in patients harboring disease-causing ALS2 mutations have not been directly evaluated, disruption of Rac function as a possible underlying cause of neurodegenerative disease is suggested by the fact that alsin mediates Rac-depen-

\* This work was supported, in whole or in part, by National Institutes of Health Grant R01 NS062766 from the NINDS (to D. A. L.). This work was also supported by a merit review award from the Department of Veterans Affairs (to D. A. L.).

<sup>†</sup> Both authors contributed equally to this work.

<sup>2</sup> To whom correspondence should be addressed: Veterans Affairs Medical Center, Research-151, 1055 Clermont St., Denver, CO 80220. E-mail: Dan.Linseman@va.gov.

<sup>3</sup> The abbreviations used are: CGN, cerebellar granule neuron; ToxB, *C. difficile* toxin B; pan-JI; pan-JAK inhibitor; pSTAT, phosphorylated STAT; CDK, cyclin-dependent kinase; Ad, adenoviral; SOCS, suppressors of cytokine signaling; GR, glucocorticoid receptor; DN, dominant negative.

## Rac Inhibition Induces STAT5-dependent Neuronal Apoptosis

dent prosurvival signaling in primary motor neurons (7). Collectively, these findings implicate Rac as a crucial mediator of neuronal survival and suggest that disruption of Rac activity may contribute to the progression of neurodegenerative disorders.

We have reported previously that inhibition of Rho GTPases with *Clostridium difficile* toxin B (ToxB) and in particular inhibition of Rac lead to the derepression of an as yet undefined proapoptotic JAK/STAT pathway (8). The JAK/STAT pathway has been shown to play a critical role in cytokine signaling, and JAK activation can turn on an array of downstream effects including cell proliferation, differentiation, and apoptosis (9). An important feature of the JAK/STAT signaling cascade is that it can exert either a prosurvival or proapoptotic effect depending upon the stimulus and cell type. For example, cytoprotective signals are transmitted from the gp130 receptor to a pro-survival JAK/STAT3 pathway in cardiac myocytes (10). Moreover, data implicate constitutive activation of STAT1 and STAT3 proteins in breast cancer cells (11). Conversely, more recent data have emerged to suggest that the JAK/STAT pathway may also induce apoptosis under certain cellular conditions. For instance, STAT1 has been shown to mediate IFN- $\gamma$ -induced apoptosis in liver cells treated with the hepatotoxic compound galactosamine (12). In addition, chromatin immunoprecipitation experiments performed in thymocytes suggest that glucocorticoids induce apoptosis through repression of prosurvival Bcl-xL in a STAT5-dependent manner (13). Although it is clear that JAK/STAT activation can induce apoptosis in diverse non-neuronal cell types, the significant involvement of this signaling pathway in neuronal apoptosis has only recently been recognized.

In a previous study, we showed that inhibition of Rac induces CGN apoptosis by inactivating a prosurvival p21-activated kinase PAK/mitogen-activated protein kinase kinase (MEK)/extracellular signal-regulated kinase (ERK) cascade. Although we have demonstrated that disruption of this pathway results in the derepression of a proapoptotic JAK/STAT pathway, we have yet to identify which particular STAT family members mediate neuronal apoptosis in response to ToxB (8). Thus, the current study focuses on identifying the STAT family members involved and the consequences of STAT activation downstream of Rac inhibition in CGNs. These primary neuronal cultures are extremely homogeneous and have been used extensively to examine molecular mechanisms involved in neuronal apoptosis (6, 14–16). Although we show that Rac inhibition leads to the up-regulation of STAT1 expression and enhanced tyrosine phosphorylation of STAT3, we report that these transcription factors are not responsible for inducing apoptosis in ToxB-treated CGNs. Instead, we demonstrate that STAT5 is activated and subsequently translocates into the nucleus to transcriptionally repress prosurvival Bcl-xL in Rac-inhibited CGNs. To our knowledge, these results are the first to identify a proapoptotic function for STAT5 in primary neurons.

### EXPERIMENTAL PROCEDURES

**Reagents**—*C. difficile* toxin B was isolated or prepared as a recombinant protein as described previously (17). The polyclonal antibodies used for immunoblotting STAT1, STAT3,

and phosphorylated STAT5 (pSTAT5) were from Cell Signaling Technology (Beverly, MA). Horseradish peroxidase-linked secondary antibodies and reagents for enhanced chemiluminescence detection were from Amersham Biosciences. The polyclonal antibody used to detect active caspase-3 by immunocytochemistry was from Promega (Madison, WI). For Western blotting, active caspase-3 was detected with a polyclonal antibody from Abcam (Cambridge, MA). 4,6-Diamidino-2-phenylindole (DAPI), Hoechst dye 33258, and a monoclonal antibody against  $\beta$ -tubulin were from Sigma. Anti-rat and anti-mouse Cy3- or FITC-conjugated secondary antibodies for immunofluorescence were from Jackson ImmunoResearch Laboratories (West Grove, PA). The monoclonal antibody against LAP-2 and the polyclonal total STAT1 and total STAT5 antibodies used for Western blotting were from BD Biosciences. Purvalanol A, JSI-124, roscovitine, mifepristone, JAK3 inhibitor, and the small molecule JAK inhibitor I (2-(1,1-dimethyl)9-fluro-3,6-dihydro-7H-benz[h]imidaz[4,5,-f]isoquinolin-7-one; pan-JAK inhibitor (pan-JI)) were from Calbiochem. The specific JAK1/2 inhibitor ruxolitinib was purchased from ChemieTek (Indianapolis, IN), and the JAK3 inhibitor tofacitinib was from Selleck Chemicals (Houston, TX).

**CGN Culture**—Rat CGNs were isolated and cultured from 7-day-old Sprague-Dawley rat pups of both sexes (15–19 g) as described previously (6). Briefly, CGNs were plated on 35-mm-diameter plastic dishes coated with poly-L-lysine at a density of  $2.0 \times 10^6$  cells/ml in basal modified Eagle's medium containing 10% fetal bovine serum, 25 mM KCl, 2 mM L-glutamine, 100 units/ml penicillin, and 100  $\mu$ g/ml streptomycin (Invitrogen). Cytosine arabinoside (10  $\mu$ M) was added to the culture medium 24 h after plating to limit the growth of non-neuronal cells. With this protocol, cultures were ~95% pure for granule neurons. In general, experiments were performed after 6–7 days in culture.

**CGN Culture from STAT1 Knock-out (KO) Mice**—STAT1 KO mice and their wild-type littermates were obtained commercially from Taconic (Hudson, NY). CGNs from these mice were isolated and cultured essentially as described above.

**Cell Lysis and Immunoblotting**—After treatment as described under "Results," CGN whole cell lysates or immune complexes of STAT5A or STAT5B were prepared for Western blotting essentially as described previously (8). Protein concentrations were determined by a commercially available protein assay kit (BCA, Thermo Scientific), and SDS-polyacrylamide gel electrophoresis was performed using equal amounts of protein followed by transfer to polyvinylidene difluoride (PVDF) membranes (Amersham Biosciences). Nonspecific binding sites were blocked in phosphate-buffered saline (PBS) (pH 7.4) containing 0.1% Tween 20 (PBS-T), 1% bovine serum albumin (BSA), and 0.01% sodium azide for 1 h at room temperature (25 °C). Membranes were incubated for 1 h in primary antibody diluted in blocking solution. Excess primary antibody was removed by washing the membranes with PBS-T five times over 25 min. The membranes were then incubated for 1 h with the appropriate horseradish peroxidase-conjugated secondary antibodies diluted in PBS-T. Excess secondary antibody was removed by washing the membranes with PBS-T five times over 25 min. Immunoreactive proteins were detected by

enhanced chemiluminescence. Blots shown are representative of a minimum of three independent experiments.

**Quantification of Apoptosis**—After induction of apoptosis, CGNs were fixed in 4% paraformaldehyde for 30 min, and nuclei were stained with Hoechst dye (8 µg/ml final concentration) for 30 min. CGNs containing condensed and/or fragmented nuclei were scored as apoptotic. Typically, ~800 cells were quantified from each 35-mm well by randomly counting five 40× fields. Final counts represent data obtained from at least three independent experiments performed in duplicate.

**Immunocytochemistry**—CGNs were plated at a density of  $2.0 \times 10^6$  cells/ml in 35-mm wells. After ToxB treatment, CGNs were fixed in 4% paraformaldehyde, washed once in PBS, and then permeabilized and blocked in PBS containing 0.2% Triton X-100 and 5% BSA. Primary antibodies were diluted in 2% BSA and 0.2% Triton X-100 in PBS, and cells were incubated in primary antibody overnight at 4 °C. Cells were subsequently washed five times in PBS and then incubated for 1 h with DAPI and either Cy3- or FITC-conjugated secondary antibody diluted in 2% BSA and 0.2% Triton X-100. The cells were washed five additional times with PBS before the addition of an antiquench solution composed of 0.1% *p*-phenylenediamine in 75% glycerol in PBS. Fluorescent images were captured using a 40× water oil immersion objective on a Zeiss Axioplan 2 microscope with a Cooke Sensicam deep cooled charge-coupled device camera and a Slidebook software analysis program for digital deconvolution (Intelligent Imaging Innovations Inc., Denver, CO).

**Preparation of Nuclear and Cytosolic Extracts from CGNs**—Nuclear and cytosolic extracts were prepared as described by Li *et al.* (18). Briefly, CGNs were detached from culture dishes by a cell scraper and centrifuged at  $250 \times g$  for 5 min. The cell pellets were washed and homogenized with 15 strokes of a tightly fitting Dounce homogenizer to release nuclei. Next, the homogenate was centrifuged at  $14,000 \times g$  for 15 s to pellet the nuclei. The supernatants (cytosolic fractions) were removed, the pellets were resuspended in a HEPES/glycerol buffer, and nuclear proteins were extracted at 4 °C for 45 min. Insoluble nuclei were precipitated by centrifugation at  $14,000 \times g$  for 15 min, and the supernatants were dialyzed against a Tris/glycerol buffer for 3 h at 4 °C.

**Adenovirus Preparation and Infection**—Wild-type STAT5 and dominant negative STAT5 adenoviral constructs were prepared as described previously (19). CGNs were infected *in vitro* on day 6 with adenovirus carrying GFP, wild-type STAT5, or dominant negative STAT5 at a multiplicity of infection of 100. At 48 h of infection, cells were treated with 40 ng/ml ToxB. At 72 h of infection, cell lysates were prepared for immunoblot analysis, or cells were fixed for immunocytochemistry as described above.

**Chromatin Immunoprecipitation (ChIP)**—ChIP assays were performed according to the manufacturer's protocol using the ChIP assay kit from Active Motif (Carlsbad, CA). CGNs were treated with 40 ng/ml ToxB for 0 and 8 h. Next, DNA-associated proteins were cross-linked with formaldehyde. Cross-linked chromatin was extracted, sheared enzymatically, and incubated with a ChIP grade STAT5 antibody overnight at 4 °C and protein G-agarose beads. After washing, immune com-

plexes were eluted from the beads, heated to reverse the cross-links, and treated with proteinase K and RNase A to remove proteins and any contaminating RNA. DNA was analyzed by polymerase chain reaction (PCR) using the following primers provided by SABiosciences that generate a 114-bp product that corresponds to the promoter region of the rat Bcl-xL gene: forward primer, 5'-GAAGCTGACACCAGTGAGTGTCCGAA-CGGTAAATGCCTACGAAGCTGACACCACTGAGTG-3'; and reverse primer, 5'-GTAGGCATTTACCGTTCGGA-3'. These primers were selected because they amplify a sequence of DNA that is near two predicted STAT5 binding sites on the promoter region of Bcl-xL variant 1 and variant 2. As a negative control, ChIP reactions were performed as described in the absence of STAT5 antibody followed by PCR. PCR was performed using the following conditions: one cycle of 95 °C for 10 min followed by 40 cycles of 95 °C for 15 s and 60 °C for 60 s.

**Data Analysis**—Results represent the mean ± S.E. for the number (*n*) of independent experiments performed. Statistical differences between the means of unpaired sets of data were evaluated by one-way analysis of variance with a post hoc Tukey's test. A *p* value of <0.05 was considered statistically significant. Images and immunoblots are representative of at least three independent experiments. For the cycle threshold values reported in Fig. 10*A*, results represent the mean for four independent experiments, and statistical differences were evaluated by a Student's *t* test.

## RESULTS

**STAT1 Is Up-regulated in JAK-dependent Manner in CGNs Treated with Rho Family GTPase Inhibitor ToxB**—To evaluate the involvement of Rac in CGN survival, cultures were incubated with *C. difficile* toxin B. This cytotoxin monoglycosylates a key threonine residue in the switch 1 region of Rho GTPases, thus preventing any interactions with downstream effectors (17, 20). We have shown previously that inhibition of the Rho family member Rac with ToxB elicits the derepression of a pro-apoptotic JAK/STAT pathway in CGNs (8). However, the specific STAT family protein involved in this pathway has not yet been elucidated. As STAT1 is the most extensively described family member in studies of apoptosis (21–23), we examined its expression following Rac inhibition. CGNs incubated with ToxB for 24 h exhibited a marked increase in the expression of STAT1 (Fig. 1*A*). Moreover, co-incubation with a small molecule pan-JI (structure shown in Fig. 1*B*) was sufficient to prevent the induction of STAT1 by ToxB, confirming that the increase in STAT1 is dependent on JAK activation (Fig. 1*A*).

In addition to provoking apoptosis in a variety of diverse cell types (24–26), activated STAT1 has been shown to play a pro-apoptotic role in neuronal death induced during ischemic brain injury (27). To determine whether derepression of a JAK/STAT1 pathway exerts a similar proapoptotic effect in Rac-inhibited neurons, we examined the neuroprotective effects of pan-JI in ToxB-treated CGNs. Examination of nuclei by Hoechst staining revealed increased apoptotic cell death in ToxB-treated CGNs as evidenced by nuclear fragmentation and/or condensation. The effect of ToxB on the morphology of CGN nuclei was significantly attenuated by co-treatment with the pan-JI (Fig. 1*D*, lower panels). As an additional means of

## Rac Inhibition Induces STAT5-dependent Neuronal Apoptosis

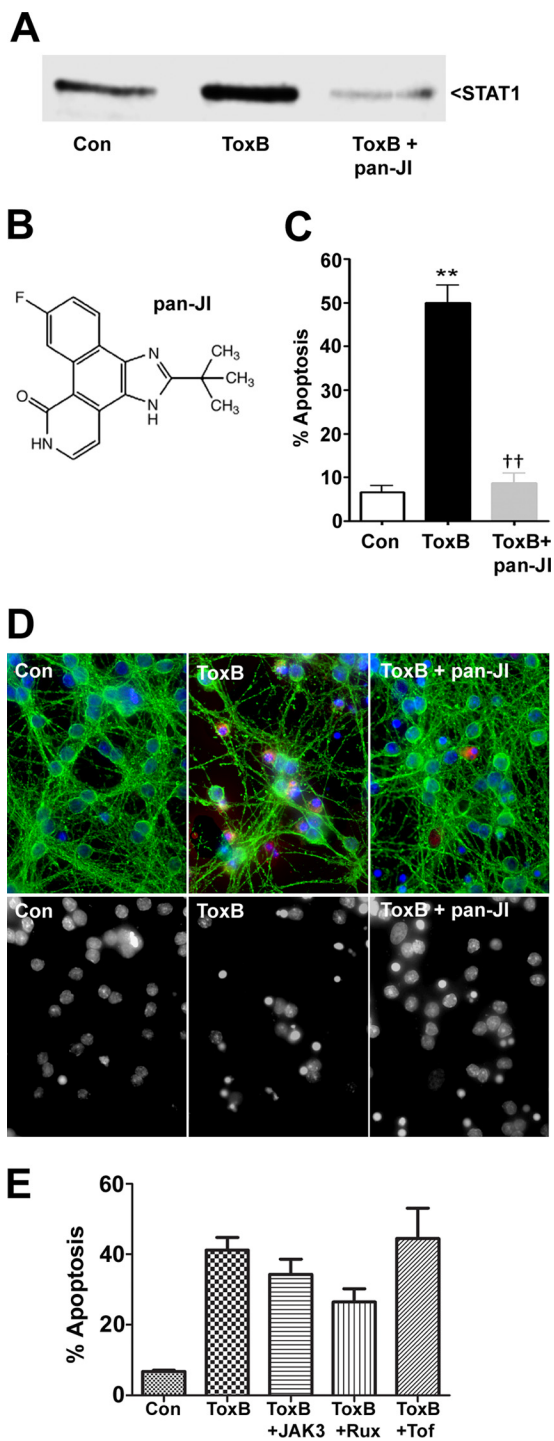


**FIGURE 1.** **STAT1 is up-regulated in JAK-dependent manner during CGN apoptosis induced by Rho family GTPase inhibitor ToxB.** *A*, CGNs were incubated for 24 h in complete medium containing 25 mM KCl and serum (control (Con) medium) ± ToxB (40 ng/ml) or ToxB + pan-JI (1  $\mu$ M). Cells were then lysed, and proteins were resolved by SDS-PAGE and transferred to PVDF membranes. The membrane was probed with an antibody against STAT1. STAT1 expression was up-regulated when treated with ToxB, and this effect was blocked by pan-JI. *B*, molecular structure of pan-JI. *C*, quantification of apoptosis in CGNs incubated for 24 h as described in *A*. \*\*,  $p < 0.01$  compared with control (Con); ††,  $p < 0.01$  compared with ToxB. *D*, CGNs were incubated for 24 h as described in *A*. For 4 independent experiments following incubation, cells were incubated with a polyclonal antibody against active caspase-3 (shown in red) and a monoclonal antibody against  $\beta$ -tubulin (shown in green), and nuclei were stained with DAPI (shown in blue). Lower panels show decolorized DAPI staining of nuclei for clarity. CGNs incubated with ToxB exhibited

identifying apoptotic cells, we examined caspase-3 activation as cleavage to its active proteolytic fragments is a hallmark of apoptosis and signifies commitment to cell death (28). CGNs treated with ToxB alone exhibited increased activation of caspase-3, and this effect was blocked by pan-JI (Fig. 1*D*, upper panels). Quantification of apoptosis in CGNs co-incubated with ToxB and pan-JI revealed that the pan-JI conferred significant neuroprotection and effectively reduced apoptosis to control levels (Fig. 1*C*). Taken together, these data suggest that inhibition of Rac with ToxB results in the activation of a pro-apoptotic JAK/STAT1 signaling pathway in CGNs.

To elucidate the specific JAK family member(s) that induces STAT activation downstream of Rac inhibition in CGNs, we evaluated the protective effects of more targeted JAK inhibitors against ToxB. We found that two specific JAK3 inhibitors (JAK3 inhibitor and tofacitinib) did not confer significant neuroprotection in ToxB-treated CGNs (Fig. 1*E*). However, we found that the JAK1/2 inhibitor (ruxolitinib) modestly protected CGNs from ToxB-mediated apoptosis, although this effect did not quite reach statistical significance. Based on the marked protective effects of the pan-JI (which inhibits JAK1–3 and Tyk2 with similar potency) and our results showing that more targeted inhibition of specific JAK family members (JAK1–3) is not overtly protective, these data suggest a possible contribution of Tyk2 in mediating the apoptosis downstream of ToxB-mediated Rac inhibition in primary CGNs.

**STAT1 Is Not Activated by Tyrosine Phosphorylation nor Does It Translocate into Nucleus of ToxB-treated CGNs**—Next, we examined the phosphorylation status and localization of STAT1 in CGNs exposed to ToxB. To translocate into the nucleus and influence gene expression, members of the STAT family must be activated via tyrosine phosphorylation (29). Whereas total STAT1 expression increased in CGNs treated for 24 h with ToxB, time course experiments performed for up to 24 h did not show significant activation of STAT1 as assessed by tyrosine phosphorylation (Fig. 2*A*). Furthermore, using immunostaining to examine STAT1 localization, we found that STAT1 remained cytosolic and perinuclear in CGNs following ToxB treatment (Fig. 2*B*). These observations are striking in that they suggest that the observed up-regulation of STAT1 expression may not be directly involved in apoptosis following ToxB-mediated inhibition of Rac.

**CGNs from STAT1 Knock-out Mice Are Susceptible to ToxB-induced Apoptosis**—To definitively establish whether the up-regulation of total STAT1 expression in the absence of enhanced tyrosine phosphorylation or nuclear translocation is involved in ToxB-mediated apoptosis, we measured the effects of ToxB on primary cultures of CGNs isolated from STAT1 KO mice versus their wild-type (WT) littermates. CGNs from WT

many condensed and/or fragmented nuclei and displayed increased immunoreactivity for active caspase-3. CGNs co-incubated with pan-JI were significantly protected from apoptosis and displayed nuclear morphology similar to that in controls. Scale bar, 10  $\mu$ m. *E*, CGNs were incubated for 24 h in control medium ± ToxB (40 ng/ml) or ToxB + JAK3 inhibitor (JAK3 Inh; 100  $\mu$ M), ruxolitinib (Rux; 10  $\mu$ M), or tofacitinib (Tof; 10  $\mu$ M). Following incubation, cells were fixed with 4% paraformaldehyde, and the nuclei were stained with Hoechst dye. Apoptotic cells were scored as those with condensed and/or fragmented nuclei. Values are mean ± S.E. for 6 independent experiments.

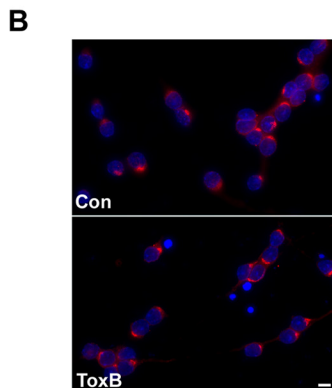
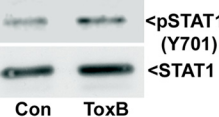
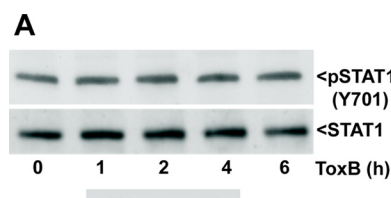


**FIGURE 2. STAT1 does not display increased tyrosine phosphorylation nor does it translocate into nucleus of ToxB-treated CGNs.** *A*, a 24-h time course of ToxB treatment (40 ng/ml) was performed in CGNs. Cell lysates were resolved by SDS-PAGE, and proteins were transferred to PVDF membranes. The blots were probed with antibodies against pSTAT1 (Tyr-701) and STAT1. Little to no increase in the tyrosine phosphorylation of STAT1 was observed in CGNs subjected to ToxB for up to 24 h. *B*, CGNs were incubated with control (Con) medium ± ToxB (40 ng/ml) for 8 h. Cells were fixed, and their nuclei were stained with DAPI. A primary antibody against pSTAT1 (Tyr-701) and a Cy3-conjugated secondary antibody were used to visualize pSTAT1. Incubation of CGNs with ToxB did not result in translocation of pSTAT1 into the nucleus. Scale bar, 10 μm.

mice demonstrated a marked increase in STAT1 expression following ToxB treatment, whereas CGNs from STAT1 KO mice did not demonstrate any expression of STAT1 in either the absence or presence of ToxB (Fig. 3A), thus confirming effective knock-out of STAT1 expression in these mice. Unexpectedly, CGNs from both WT and STAT1 KO mice equally succumbed to apoptosis in response to ToxB treatment (Fig. 3B), whereas inclusion of the pan-JI was equally neuroprotective for both cell types (Fig. 3C). Collectively, these data indicate that although total STAT1 is up-regulated a different member of the STAT family mediates JAK-dependent apoptosis in Rac-inhibited CGNs.

**STAT3 Is Tyrosine Phosphorylated in Response to ToxB, and This Effect Is Blocked by Pan-JI**—As our data demonstrate that STAT1 up-regulation does not significantly contribute to apoptosis in Rac-inhibited CGNs, we next evaluated the involvement of additional members of the STAT family. Recent evidence suggests that STAT3 mediates β-amyloid-induced apoptosis in mouse cortical neurons (30). To determine whether ToxB-targeted inhibition of Rac acts to ultimately activate a similar proapoptotic JAK/STAT3 pathway, we analyzed the activation of STAT3 in response to ToxB treatment. Time course experiments demonstrated that STAT3 was tyrosine phosphorylated as early as 6 h after ToxB treatment (Fig. 4A),

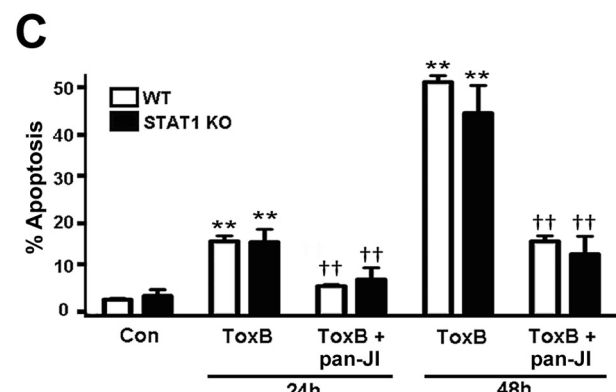
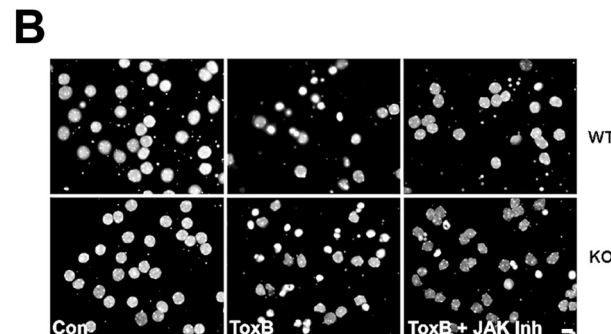
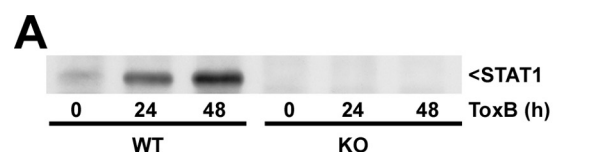


**FIGURE 3. CGNs from STAT1 knock-out and wild-type mice are equally susceptible to ToxB-induced apoptosis.** *A*, CGNs from WT and STAT1 KO mice were treated for 0, 24, or 48 h with ToxB (40 ng/ml). Cell lysates were resolved by SDS-PAGE, and proteins were transferred to PVDF membranes. The blot was probed with a primary antibody against STAT1. The Western blot shows induced expression of STAT1 in WT CGNs after treatment with ToxB. *B*, WT and STAT1 KO CGNs were incubated for 48 h in control (Con) medium ± ToxB (40 ng/ml) or with ToxB + pan-JI (1 μM). Cells were fixed, and nuclei were stained with Hoechst. Both WT and KO cells treated with ToxB displayed condensed and/or fragmented nuclear morphology. WT and KO CGNs co-incubated with pan-JI exhibited nuclear morphologies similar to those of control cells. Scale bar, 10 μm. *C*, quantification of apoptosis in CGNs incubated for 24 or 48 h with control medium ± ToxB (40 ng/ml) or ToxB + pan-JI (1 μM). STAT1 KO cells succumbed to apoptosis as readily as WT CGNs after treatment with ToxB. When co-incubated with pan-JI, STAT1 KO and WT CGNs showed similar protection from ToxB. \*\*, p < 0.01 compared with control; ††, p < 0.01 compared with ToxB. Inh, inhibitor. Values are mean ± S.E. for 3 independent experiments.

and inclusion of pan-JI blocked the phosphorylation of STAT3 at both 6 and 8 h in ToxB-treated CGNs (Fig. 4B).

**Reputed STAT3 Inhibitor JSI-124 Protects CGNs from ToxB-induced Apoptosis**—To further define the potential role of STAT3 in the proapoptotic pathway activated downstream of Rac inhibition, we examined whether or not the reputed STAT3 inhibitor JSI-124 (31) exerted a protective effect in ToxB-treated CGNs (Fig. 5A). Following a 24-h incubation period with ToxB alone, many CGNs displayed condensed and/or fragmented nuclei consistent with apoptosis. In contrast, CGNs co-incubated with JSI-124 were essentially completely protected from apoptosis, and their nuclei were morphologically similar to those in control cells (Fig. 5B). Inclusion of JSI-124 reduced CGN apoptosis in the presence of ToxB to

## Rac Inhibition Induces STAT5-dependent Neuronal Apoptosis

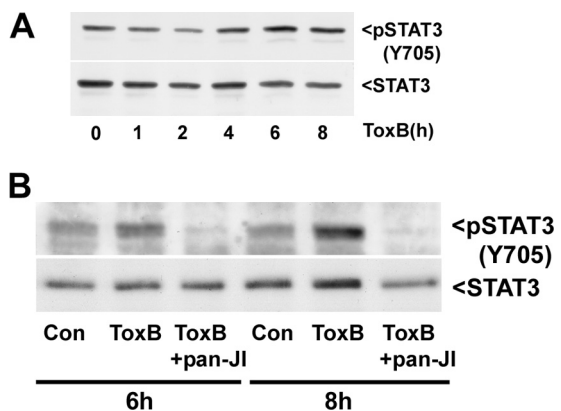


**FIGURE 4.** **STAT3 is tyrosine phosphorylated in response to ToxB in CGNs, and this effect is blocked by pan-JI.** *A*, CGNs were incubated for various periods of time up to 8 h with ToxB in control medium. Cells were lysed, and proteins were resolved by SDS-PAGE and transferred to PVDF membranes. The blot was probed with antibodies against pSTAT3 (Tyr-705) or STAT3. The expression of pSTAT3 increased in response to ToxB. *B*, CGNs were incubated for 6 or 8 h in control (Con) medium ± ToxB (40 ng/ml) or ToxB + pan-JI (1  $\mu$ M). Cell lysates were resolved by SDS-PAGE, and proteins were transferred to PVDF membranes. The blot was probed with antibodies against pSTAT3 (Tyr-705) or STAT3. The pan-JI inhibitor blocked ToxB-induced STAT3 phosphorylation.

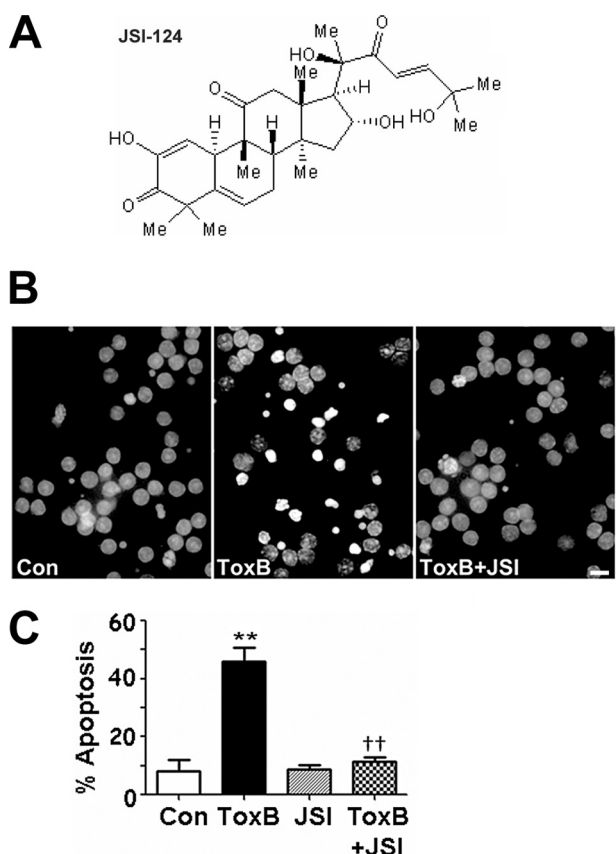
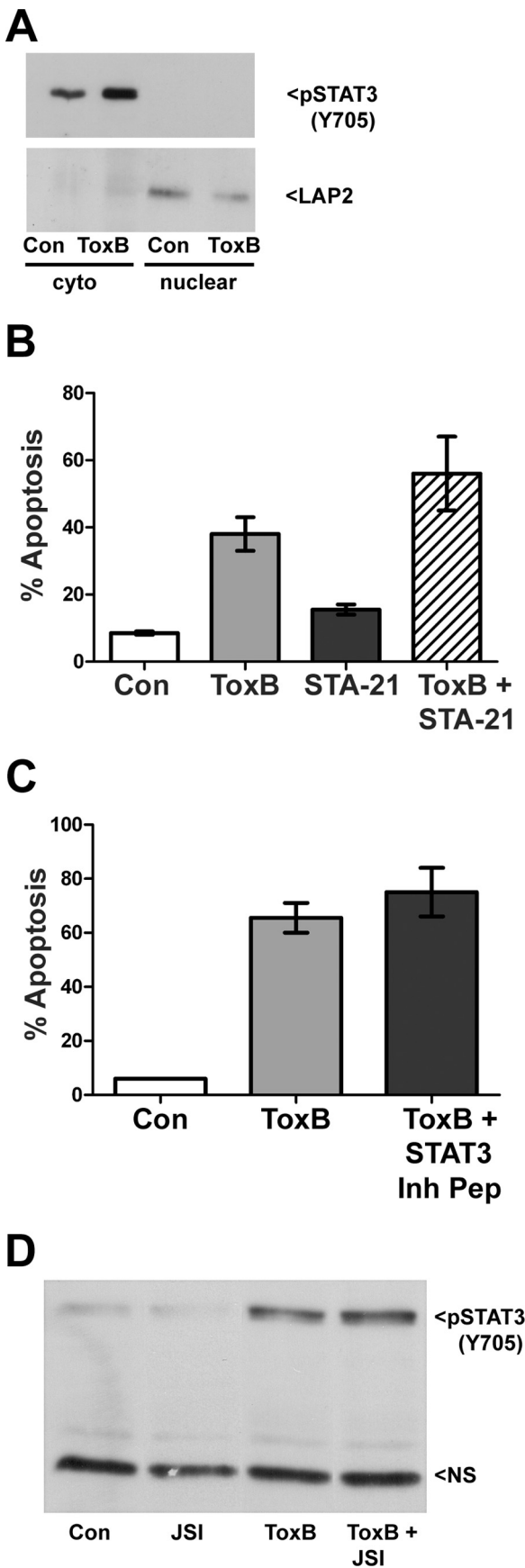


**FIGURE 5.** **A reputed STAT3 inhibitor, JSI-124, protects CGNs from ToxB-induced apoptosis.** *A*, molecular structure of JSI-124. *B*, CGNs were incubated for 24 h in control (Con) medium ± ToxB (40 ng/ml) or ToxB + JSI-124 (JSI; 5  $\mu$ M). Cells were fixed, and their nuclei were stained with Hoechst dye. CGNs treated with ToxB exhibited significantly more condensed and/or fragmented nuclei than control CGNs. CGNs co-incubated with JSI-124 were significantly protected from apoptosis, and their nuclei were morphologically similar to those of control cells. Scale bar, 10  $\mu$ m. *C*, quantification of apoptosis in CGNs treated with ToxB or ± JSI-124. Values are mean ± S.E. JSI-124 significantly protected CGNs from ToxB-induced apoptosis. \*\*,  $p < 0.01$  compared with control; ††,  $p < 0.01$  compared with ToxB. Values are mean ± S.E. for 5 independent experiments.

~10% (Fig. 5C). These data support a model in which a proapoptotic JAK/STAT3 pathway mediates apoptosis in Rac-inhibited CGNs.

**Phosphorylated STAT3 Does Not Translocate into Nucleus of CGNs following Treatment with ToxB, and Additional STAT3 Inhibitors Do Not Protect CGNs from Apoptosis Induced by ToxB**—To further investigate the role of STAT3 in apoptosis, we examined whether or not pSTAT3 translocates into the nucleus following ToxB treatment. Nuclear fractionation experiments demonstrated that although STAT3 was tyrosine phosphorylated pSTAT3 remained cytosolic following ToxB targeted inhibition of Rac (Fig. 6A). Furthermore, two additional STAT3 inhibitors, STA-21 and a STAT3 inhibitory peptide, did not protect CGNs from ToxB-induced apoptosis (Fig. 6, *B* and *C*). These results indicate that STAT3 does not directly regulate apoptosis downstream of Rac inhibition. This finding was particularly surprising as the selective STAT3 inhibitor JSI-124 exerted a neuroprotective effect in ToxB-treated CGNs. However, further evaluation of the effects of JSI-124 in CGNs revealed that this compound in fact had no significant inhibitory effect on ToxB-induced STAT3 phosphorylation (Fig. 6D). These data suggest that the mechanism by which JSI-124 protects CGNs from apoptosis is unrelated to attenuation of activated STAT3 and may involve a different member of the STAT family.

**Tyrosine Phosphorylation of STAT5 in Response to ToxB in CGNs Is Blocked by JSI-124 and Putative STAT5 Inhibitor Roscovitine**—Recent evidence demonstrates a necessary role for STAT5 in apoptosis induced by oncostatin M in osteosarcoma cells (32). In addition, both STAT5 isoforms have been implicated in the down-regulation of the prosurvival Bcl-xL protein in thymocytes (33). Therefore, we next examined STAT5 and found that STAT5 was tyrosine phosphorylated in ToxB-treated CGNs. Interestingly, although blotting for total STAT5 clearly showed the presence of both STAT5A (94 kDa) and STAT5B (92 kDa) in CGNs (Fig. 7A, *lower blot*), Western blots for phospho-STAT5 only indicated a single tyrosine phosphorylated isoform in response to ToxB (Fig. 7A, *upper blot*). Therefore, we next sought to determine whether STAT5A or STAT5B was phosphorylated in response to ToxB. To establish which STAT5 isoform was phosphorylated, we compared lysates that were immunoprecipitated for either STAT5A or STAT5B with whole cell lysates and Western blotted for total STAT5. Using this approach, we were able to determine where the STAT5A and STAT5B isoforms were detected by immunoblot (Fig. 7B, *left panel*). Despite efficient immunoprecipitation of each of the STAT5 isoforms from CGNs using isoform-specific antibodies, we were not able to observe tyrosine phosphorylation of either isoform in response to ToxB. However, in whole cell lysates obtained following 8 h of ToxB treatment, we observed a pronounced increase in the tyrosine phosphorylation of the higher molecular weight STAT5A isoform but not STAT5B using a phosphospecific antibody to STAT5 (Fig. 7B, *right panel*). The inability to observe STAT5A tyrosine phosphorylation following immunoprecipitation may reflect the physical association of STAT5A with one or more protein tyrosine phosphatases, any one of which may be insensitive to the phosphatase inhibitors present in our lysis buffer, as described



previously (34, 35). Our data are consistent with several previous reports demonstrating that STAT5A and STAT5B can be individually activated in a stimulus- and cell type-specific manner (36–40).

In addition, co-treatment of CGNs with either JSI-124 or the putative STAT5 inhibitor roscovitine (54) was sufficient to block the tyrosine phosphorylation of STAT5A in response to ToxB (Fig. 7, A and B). To further substantiate the involvement of STAT5 in ToxB-treated CGNs, we examined STAT5 phosphorylation and localization by immunocytochemistry. In control CGNs, the expression of pSTAT5 detected by immunofluorescence was negligible. In contrast, following incubation of CGNs with ToxB, there was a profound increase in the immunoreactivity for pSTAT5, and this transcription factor was principally localized to CGN nuclei (Fig. 7C). Collectively, these data indicate that STAT5 is tyrosine phosphorylated in response to ToxB and localizes to the nucleus under these conditions to modulate gene transcription. Moreover, the tyrosine phosphorylation of STAT5 appears to be specific for the STAT5A isoform and is sensitive to inhibition by either JSI-124 or roscovitine.

**Roscovitine Significantly Protects CGNs from ToxB-induced Apoptosis**—Consistent with STAT5 playing a key role in ToxB-induced apoptosis, CGNs co-treated with ToxB and roscovitine displayed healthy, intact nuclei (Fig. 8A). Quantification of these results shows that roscovitine significantly protected CGNs from ToxB-induced apoptosis (Fig. 8B). In addition, ToxB treatment for 24 h resulted in the cleavage of pro-caspase-3 to its active fragments, an effect largely attenuated by roscovitine (Fig. 8C). Generally, roscovitine is used to suppress the cell cycle through inhibition of cyclin-dependent kinases (CDKs) (41). To ensure that the protection conferred by roscovitine was not through CDK suppression but was a result of STAT5 inhibition, CGNs were also treated with ToxB ± purvalanol A, a closely related CDK inhibitor. Although remarkably similar in structure, purvalanol A did not protect CGNs from ToxB-induced apoptosis and in fact significantly enhanced cell death (Fig. 8D). These results suggest that the neuroprotective effects of roscovitine are unrelated to CDK suppression and are likely due to STAT5 inhibition.

**FIGURE 6. Phosphorylated STAT3 does not translocate into nucleus of CGNs following treatment with ToxB, and additional STAT3 inhibitors do not protect CGNs from apoptosis.** *A*, CGNs were incubated in control (Con) medium ± ToxB (40 ng/ml) for 8 h. Following incubation, the cells were fractionated into nuclear and cytosolic (cyto) fractions as described under “Experimental Procedures.” A monoclonal antibody against pSTAT3 (Tyr-705) was used for Western blotting. pSTAT3 did not translocate into the nucleus following treatment with ToxB. The purity of the nuclear fractions was verified by immunoblotting for LAP-2. *B*, CGNs were incubated for 24 h in control medium ± ToxB (40 ng/ml) or ToxB + STA-21 (20  $\mu$ M). Cells were fixed, and nuclei were stained with Hoechst dye to quantify apoptosis. STA-21 did not protect CGNs from ToxB-induced apoptosis. Results shown are mean  $\pm$  range ( $n = 2$ ). *C*, CGNs were incubated for 24 h in control medium ± ToxB (40 ng/ml) or ToxB + STAT3 inhibitory peptide (Inh Pep; 100  $\mu$ M). Cells were fixed, and nuclei were stained with Hoechst dye to quantify apoptosis. STAT3 inhibitory peptide did not protect CGNs from ToxB-induced apoptosis. Results shown are mean  $\pm$  range ( $n = 2$ ). *D*, CGNs were incubated for 24 h in control medium ± ToxB (40 ng/ml), JSI-124 (JSI; 5  $\mu$ M), or ToxB + JSI-124. The cells were lysed, and proteins were separated by SDS-PAGE and transferred to PVDF membranes. Blots were probed for pSTAT3 (Tyr-705). ToxB increased the expression of pSTAT3. This effect was not blocked by co-incubation with JSI-124. NS, nonspecific band shown to indicate equal protein loading. Values are mean  $\pm$  range for 2 independent experiments.

## Rac Inhibition Induces STAT5-dependent Neuronal Apoptosis

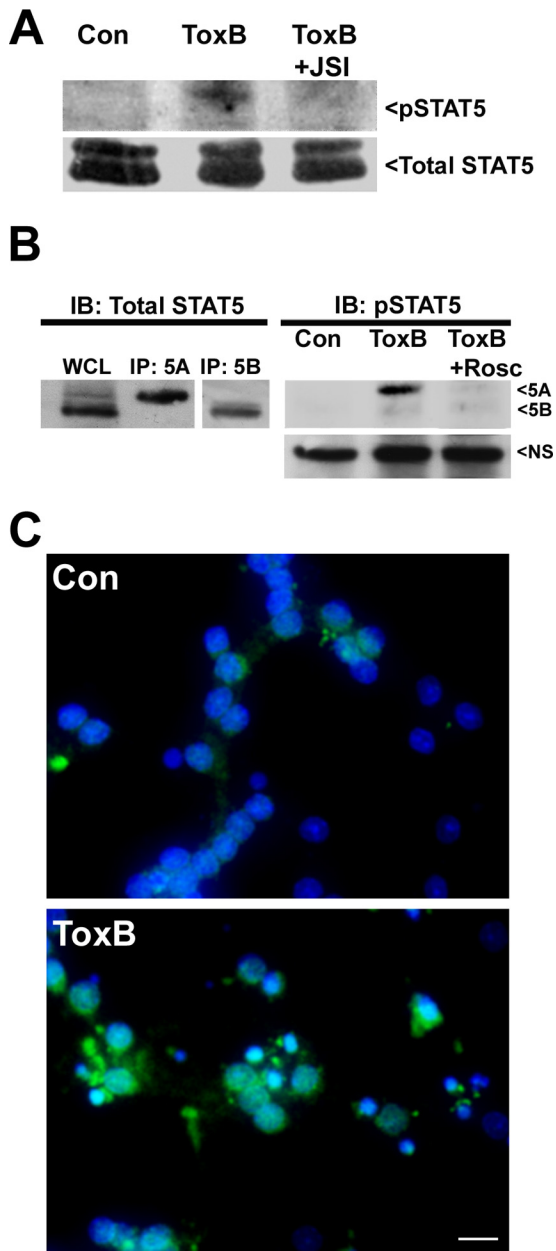


**FIGURE 7.** STAT5A shows enhanced tyrosine phosphorylation in response to ToxB in CGNs that is blocked by JSI-124 and STAT5 inhibitor roscovitine. *A*, CGNs were incubated in control (Con) medium ± ToxB (40 ng/ml) or ToxB + JSI-124 (JSI; 5  $\mu$ M) for 24 h. Cells were lysed, and proteins were resolved by SDS-PAGE and transferred to PVDF membranes. Blots were probed for pSTAT5 (Tyr-694) and total STAT5. STAT5 was phosphorylated in response to ToxB, and this effect was blocked by JSI-124. *B*, CGNs were incubated in control medium ± ToxB (40 ng/ml) or ToxB + roscovitine (Rosc; 30  $\mu$ M) for 24 h. Following incubation, cells were lysed and immunoprecipitated (IP; right panel) for either total STAT5A or STAT5B. Immunoprecipitated proteins and a lane containing the whole cell lysate (WCL) were resolved by SDS-PAGE and transferred to PVDF membranes. Blots were probed for pSTAT5 (Tyr-694) and total STAT5. STAT5 was phosphorylated in response to ToxB, and this effect was blocked by roscovitine. NS, nonspecific band shown to indicate equal protein loading; 5A, STAT5A; 5B, STAT5B. *C*, CGNs were incubated in control medium ± ToxB (40 ng/ml) for 24 h. Cells were fixed and incubated with a polyclonal antibody against pSTAT5 (Tyr-694; shown in green). Nuclei were stained with DAPI (shown in blue). pSTAT5 translocated into the nucleus in response to ToxB. Scale bar, 10  $\mu$ m. IB, immunoblotted.

**Adenoviral Dominant Negative STAT5 Protects CGNs from ToxB-induced Apoptosis**—As a more specific approach to definitively establish the proapoptotic role of STAT5 following disruption of Rac activity, we examined the neuroprotective effects of a dominant negative mutant of STAT5 containing a C-terminal truncation at residue 713 that removes the entire transcriptional activation domain of STAT5 (Ad-DN STAT5; Ref. 42). First, adenoviruses expressing either WT STAT5 or DN STAT5 were grown and overexpressed in HEK293AD cells, and these cells were compared with cells that were infected with the Ad-GFP control. Infection with Ad-WT STAT5 increased expression of full-length STAT5, and Ad-DN STAT5 appeared as a lower molecular weight form of STAT5 (Fig. 9A). Next, we infected CGNs with the Ad-GFP control, WT STAT5, and DN STAT5 and observed similar high level expression of the constructs (Fig. 9B). Importantly, none of the adenoviral constructs induced any significant increase in basal apoptosis of CGNs on their own (Fig. 9C). As we have consistently shown, ToxB treatment resulted in condensed and fragmented nuclei indicative of apoptosis. Not unexpectedly, preincubation of CGNs with WT STAT5 did not confer neuroprotection from ToxB treatment (Fig. 9E). However, CGNs preincubated with Ad-DN STAT5 and subsequently treated with ToxB displayed nuclear morphology strikingly more similar to that of control CGNs (Fig. 9E). Quantification of apoptosis revealed that inhibiting the transcriptional activity of endogenous STAT5 through overexpression of Ad-DN STAT5 significantly protected CGNs from ToxB-induced apoptosis (Fig. 9D). The protective effect of Ad-DN STAT5 was not as complete as that with the chemical JAK/STAT inhibitors used previously. This was likely a reflection of the infection efficiency of CGNs, which we observed to be ~50–60% in cells infected with Ad-GFP. These data highlight a novel proapoptotic function for STAT5 downstream of Rac inhibition in primary cerebellar neurons.

**STAT5 Transcriptionally Represses Bcl-xL during ToxB-induced Apoptosis**—Recent studies suggest that under certain conditions STAT5 transcriptionally represses prosurvival members of the Bcl-2 family (32, 33, 43). Disturbances in the ratio of these proteins to their corresponding proapoptotic family members can induce apoptosis. The prosurvival members of the Bcl-2 family have an important and well documented role in promoting cell survival through binding and inactivating the proapoptotic members of their same family (44). To evaluate whether STAT5 similarly represses Bcl-2 family proteins in Rac-inhibited CGNs, we isolated and purified DNA with a ChIP grade antibody to STAT5 in control CGNs or those treated with ToxB for 8 h. There was no significant difference between STAT5 bound to the promoter region of Bcl-2 in control versus ToxB-treated CGNs (data not shown). In the case of Bcl-xL, the input levels of Bcl-xL promoter DNA amplified from the non-immunoprecipitated control and ToxB-treated CGNs were not significantly different. However, the cycle threshold values obtained for amplification of the Bcl-xL promoter from STAT5 ChIP samples were significantly lower for ToxB treatment compared with the control, indicating a significant increase in STAT5 binding to the Bcl-xL promoter in Rac-inhibited CGNs (Fig. 10A). Indeed, we report that there was an apparent although not statistically significant  $9.5 \pm 4.1$

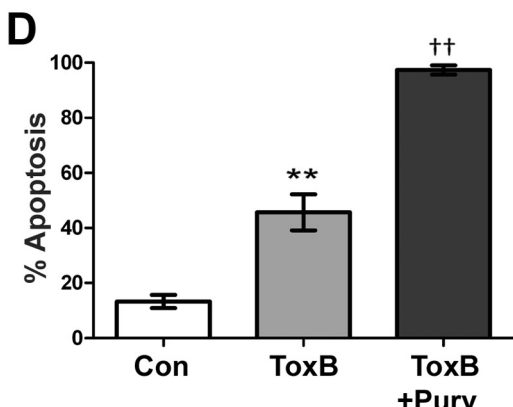
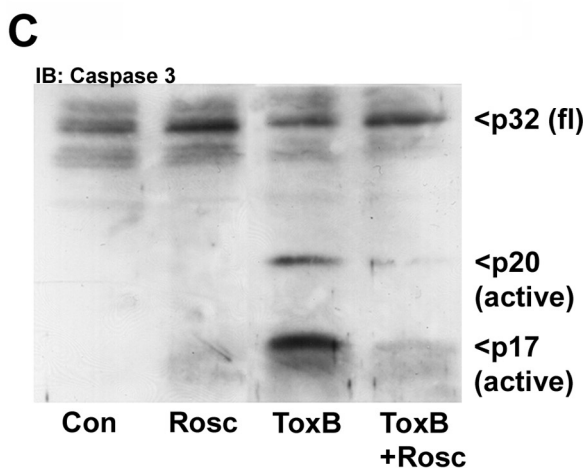
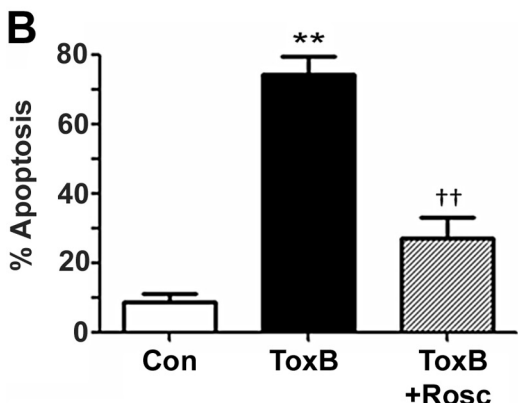
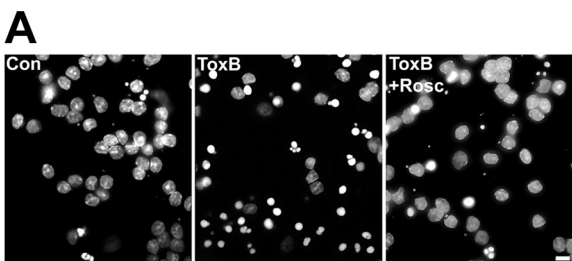


**FIGURE 8. Roscovitine significantly protects CGNs from ToxB-induced apoptosis.** *A*, CGNs were incubated for 24 h in control (Con) medium ± ToxB (40 ng/ml) or ToxB + Roscovitine (Rosc; 30  $\mu$ M). Following incubation, cells were fixed, and the nuclei were stained with Hoechst dye. Scale bar, 10  $\mu$ m. *B*, quantification of apoptosis in CGNs treated with ToxB alone or co-treated with roscovitine. Values are mean  $\pm$  S.E. ( $n = 6$ ). Roscovitine significantly protected CGNs from ToxB-induced apoptosis. \*\*,  $p < 0.01$  compared with control; ††,  $p < 0.01$  compared with ToxB. *C*, CGNs were treated as described

( $n = 4$ )-fold increase in STAT5 recruitment to the Bcl-xL promoter in response to ToxB treatment after 8 h (Fig. 10*B*). Consistent with these data, Bcl-xL expression was down-regulated at 16 h and more significantly at 24 h after ToxB treatment (Fig. 10*C*). In agreement with a relatively slow mechanism of death due to the transcriptional repression of Bcl-xL, we report that ToxB did not induce caspase-3 activation or significant apoptotic morphology until  $\sim$ 16 h of incubation after STAT5 is bound to the promoter region of Bcl-xL in CGNs (Fig. 10, *B* and *C*).

## DISCUSSION

Several studies have demonstrated a critical role for Rho GTPases (*i.e.* Rac, Rho, and Cdc42) in promoting neuronal survival (45–47). Consistent with these findings, we have shown previously that Rac activity is critical for the survival of primary CGNs (6), and Rac signaling functions to repress a proapoptotic JAK/STAT pathway in these neurons (8). Similarly, studies from other groups support a role for the activation of a pro-death JAK/STAT pathway in neurons (48, 49). For instance, Takagi *et al.* (27) reported that STAT1 was phosphorylated on activating tyrosine and serine residues and translocated into neuronal nuclei following ischemic brain injury in mice. Moreover, STAT1 KO mice displayed a decrease in the volume of ischemic brain injury and reduced TUNEL staining when compared with WT mice subjected to middle cerebral artery occlusion. Thus, STAT1 can play a proapoptotic role in neurons exposed to ischemic stress. In a similar manner, cortical neurons cultured from STAT1 KO mice showed marked resistance to interferon  $\gamma$ -stimulated neurotoxicity of the human immunodeficiency virus type 1 proteins gp120 and Tat (50). A more recent study demonstrated that exposure of SH-SY5Y neuroblastoma cells to interferon  $\beta$  induced STAT1 tyrosine phosphorylation and caspase-dependent apoptosis (51). Both STAT1 activation and caspase activation were prevented by a JAK inhibitor. Similar to STAT1, STAT3 also has the potential to have a proapoptotic effect in neurons under certain conditions. Wan *et al.* (30) recently showed that a proapoptotic Tyk2/STAT3 pathway mediates  $\beta$ -amyloid peptide-induced neuronal death. Specifically, siRNA knockdown of STAT3 protected PC12 cells from  $\beta$ -amyloid, and a STAT3 inhibitory peptide protected cultured cortical neurons. Finally, cortical neurons isolated from Tyk2-null mice were significantly less sensitive than WT neurons to  $\beta$ -amyloid-induced apoptosis. Collectively, these studies demonstrate that both STAT1 and STAT3 have the potential of acting as proapoptotic mediators in neurons under specific pathological conditions. In contrast to these previous reports, we found that although total STAT1 levels are up-regulated and STAT3 is activated via tyrosine phosphorylation in response to ToxB neither transcription factor is responsible for the neuronal apoptosis induced in CGNs by inhibition of Rac function.

in *A* and lysed. Proteins were separated by SDS-PAGE and transferred to PVDF membranes. The membrane was immunoblotted (IB) for caspase-3. Roscovitine blocked the ToxB-induced processing of caspase-3 to its active fragments. *fl*, full length. *D*, CGNs were incubated for 24 h in control medium ± ToxB (40 ng/ml) or ToxB + purvalanol A (Purv; 30  $\mu$ M). Following incubation, cells were fixed with 4% paraformaldehyde, and the nuclei were stained with Hoechst dye. Purvalanol A did not protect CGNs from ToxB-induced apoptosis. Values are mean  $\pm$  S.E. for 3 independent experiments.

## Rac Inhibition Induces STAT5-dependent Neuronal Apoptosis

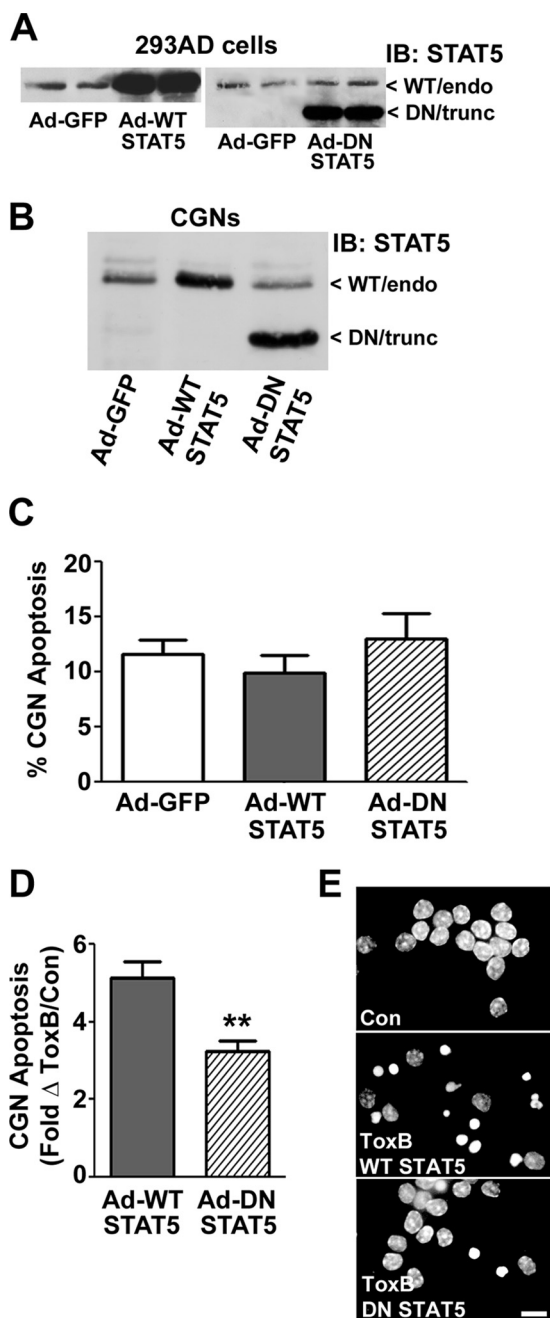


**FIGURE 9.** Adenoviral dominant negative STAT5 protects CGNs from ToxB-induced apoptosis. *A*, HEK293AD cells were infected for 48 h with an adenovirus carrying GFP (Ad-GFP), wild-type STAT5 (Ad-WT STAT5), or dominant negative STAT5 (Ad-DN STAT5). Cell lysates were separated by SDS-PAGE, transferred to PVDF membranes, and immunoblotted (*IB*) for STAT5 expression. There was a marked increase in STAT5 expression in HEK cells infected with either Ad-WT or Ad-DN STAT5. *Endo*, endogenous; *trunc*, truncated. *B*, CGNs were infected for 48 h with the same adenoviruses as described in *A*, and cell lysates were probed for STAT5 expression. *C*, CGNs were incubated for 48 h with adenoviruses as described above. The cells were fixed, and the nuclei were stained with Hoechst. Apoptotic cells were scored as those with condensed and/or fragmented nuclei. There was no significant difference in basal apoptosis in CGNs infected with Ad-GFP, Ad-WT STAT5, or Ad-DN STAT5. *D*, CGNs were infected for 48 h with either Ad-WT STAT5 or Ad-DN STAT5. After the initial 24 h of incubation, each experimental condition was treated  $\pm$  ToxB (40 ng/ml) for 24 h. At the end of the incubation, cells were fixed, and nuclei were stained with DAPI. Apoptotic cells were scored as those with condensed and/or fragmented nuclei. The fold change in apoptosis for ToxB-treated cells versus control (Con) cells was quantified. CGNs incubated with dominant negative STAT5 were protected from ToxB-induced apoptosis. Data shown represent the mean  $\pm$  S.E. for  $n = 3$  experiments.

Instead, we report that ToxB induces the enhanced tyrosine phosphorylation of STAT5, which subsequently translocates into the nucleus of CGNs. Interestingly, we found that the phosphorylation of STAT5 was prevented by the reputed STAT3 inhibitor JSI-124. This finding is perhaps not surprising given that JSI-124 has been reported to exert effects outside of STAT3 inhibition (52). In fact, this compound was recently shown to inhibit the neuroprotective effects of growth hormone against glutamate-induced toxicity in hippocampal neurons, an effect that is dependent on STAT5 activity (53). In addition to the neuroprotective effects of JSI-124, we report that roscovitine similarly inhibits STAT5 phosphorylation induced by ToxB and protects CGNs against ToxB targeted Rac inhibition. The effects of roscovitine were dissociated from its effects as a CDK inhibitor because the similarly structured compound purvalanol A did not protect CGNs from ToxB. Our data with roscovitine are consistent with a previous study showing its ability to suppress STAT5 activation in a leukemia cell line (54). Finally, we show that adenoviral infection with a dominant negative mutant of STAT5, but not WT STAT5, significantly protects CGNs from Rac inhibition with ToxB. To our knowledge, these findings are novel in that they are the first to identify a proapoptotic function for STAT5 in neurons.

Our data indicate that of the two STAT5 isoforms only STAT5A is activated via phosphorylation in CGNs exposed to ToxB-mediated Rac blockage. Although the two isoforms are highly homologous, this is consistent with several previous reports that have revealed isoform-specific STAT5 activation. Similar to our results in CGNs, JAK/STAT signaling has been shown to induce caspase-dependent apoptosis in response to granulocyte-macrophage colony-stimulating factor (GM-CSF) in OCIM2 acute myeloid leukemia cells (36). However, although GM-CSF has been shown to preferentially activate STAT5A in human monocytes (37), this factor was shown to induce specific STAT5B signaling in human neutrophils (38). In a similar manner, insulin was demonstrated to activate STAT5B, but not STAT5A, in Kym-1 rhabdomyosarcoma cells (39). Furthermore, targeted gene disruptions of either STAT5A or STAT5B in mice have shown functional differences *in vivo*. For example, deletion of STAT5A disrupts prolactin-derived mammary gland maturation, whereas disruption of STAT5B diminishes growth hormone effects on hepatic function and body mass in male mice (40). Thus, our data are consistent with several previous reports highlighting isoform-specific activation and functions of STAT5.

STAT5 is activated by many diverse cytokines and growth factors, and it is well established that this transcription factor has an important role throughout the body. Although few studies have examined the role of STAT5 in the central nervous system, the majority of reports are paradoxical to our present study and suggest that STAT5 chiefly exerts a prosurvival effect in neurons. For example, STAT5 is required in conjunction with Akt to mediate the neurotrophic and neuroprotective

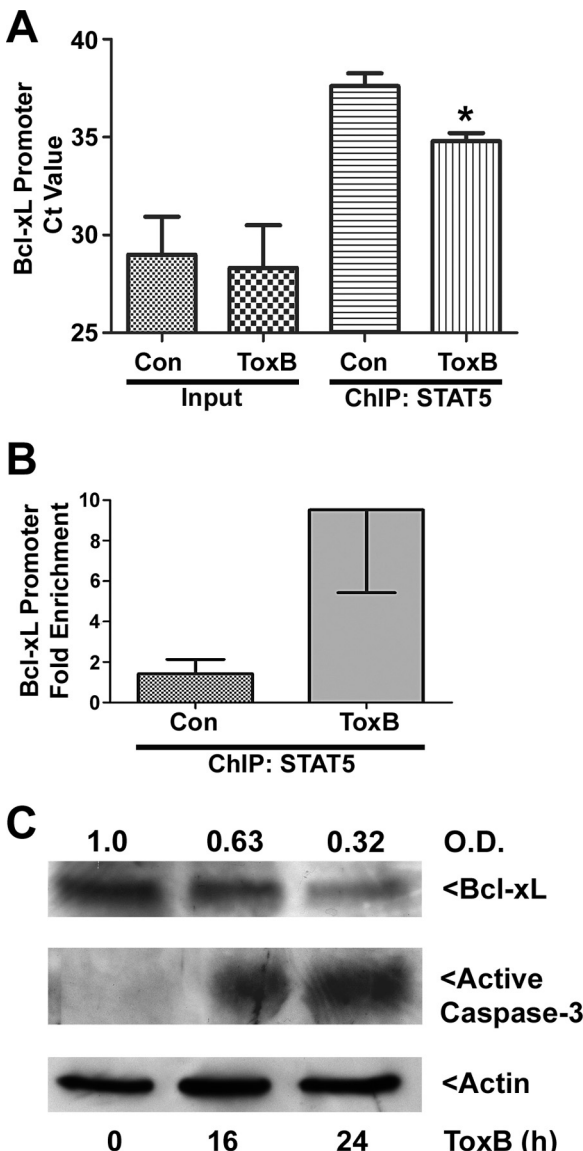


**FIGURE 10.** STAT5 transcriptionally represses Bcl-xL during ToxB-induced apoptosis. *A*, CGNs were incubated in control (Con) medium ± ToxB (40 ng/ml) for 8 h. As a control for ChIP experiments ("Input"), ChIP-quantitative PCR was performed as described under "Experimental Procedures" in the absence of the STAT5 antibody to determine the total concentration of input Bcl-xL promoter DNA. The graph shows the mean ± S.E. of the results of four independent experiments. The concentration of input DNA did not differ significantly between the control and ToxB samples. *ChIP: STAT5*, CGNs were incubated in control medium ± ToxB (40 ng/ml) for 8 h. The relative binding of STAT5 to the Bcl-xL promoter was assessed via ChIP-quantitative PCR analysis as described under "Experimental Procedures." The graph shows the mean ± S.E. of the results for four independent experiments. STAT5 binding to the Bcl-xL promoter was significantly increased in response to ToxB treatment for 8 h. \*,  $p < 0.05$  versus control evaluated by a two-tailed Student's *t* test. *B*, the -fold enrichment of STAT5 recruitment to the Bcl-xL promoter was quantified from the cycle threshold (Ct) value. STAT5 binding to the promoter region of Bcl-xL increased  $9.5 \pm 4.1$ -fold in response to 8-h ToxB treatment, although it was not statistically significant. *C*, CGNs were incubated for 0, 16, and 24 h with ToxB (40 ng/ml). Cells were then lysed, and proteins were resolved by SDS-PAGE and transferred to PVDF membranes. The membrane was probed with an antibody against Bcl-xL. Subsequently, the blot was stripped and reprobed for active caspase-3 and actin (loading control). Bcl-xL expression decreased in response to ToxB, and active caspase-3 expression increased. The values above the Bcl-xL blot represent optical densities (O.D.) of the Bcl-xL expression. The normalized optical density for the time "0" control was set to 1.0. Values are mean ± S.E. for 3 independent experiments.

effects of both growth hormone in hippocampal neurons (53) and erythropoietin in differentiated neuroblastoma cells (55). Furthermore, STAT5 was shown to elicit a prosurvival effect via induction of Bcl-2 and Bcl-xL in neural progenitor cells subjected to apoptotic stimulation (56). Thus, the relatively few studies conducted on STAT5 in neuronal models indicate that it mainly functions to transmit prosurvival signals. However, critical studies in non-neuronal cells suggest that the downstream effects of STAT5 are much more complex. STAT5 sensitizes osteosarcoma cells to apoptosis following treatment with oncostatin M (32). Moreover, in a mouse model of familial amyotrophic lateral sclerosis, a JAK3 inhibitor was shown to extend the lifespan of mutant mice when compared with those that did not receive the inhibitor. Although the effects of this inhibitor on the activation of specific STAT family members was not evaluated in this particular study, JAK3 has been shown to activate STAT5 in various studies (57–59). In evaluating various JAK isoform-selective inhibitors, we did not observe any significant inhibition of ToxB-induced apoptosis in CGNs except with a pan-JI. Thus, our data suggest a possible contribution of Tyk2 or multiple JAK isoforms in the apoptosis of neurons subjected to Rac inhibition. In conjunction with our present findings, these previous studies suggest that STAT5 functions in a cell type- and stimulus-specific manner, and the specific role of JAK/STAT5 in the central nervous system and in particular with respect to neuronal survival is likely determined by many factors.

Although we have identified Rac as a repressor of a proapoptotic JAK/STAT5 pathway, the mechanism of STAT5 activation following Rac inhibition remains incompletely understood. Suppressors of cytokine signaling (SOCS) exist as endogenous STAT inhibitors (60, 61), and previous evidence suggests that SOCS protein expression can be regulated by ERK (62, 63). This is consistent with our previous finding that a prosurvival MEK/ERK pathway functions downstream of Rac GTPase to actively repress proapoptotic JAK/STAT signaling in healthy CGNs (8). Whether SOCS proteins are indeed mediators of the Rac-dependent repression of proapoptotic JAK/STAT signaling in neurons remains to be investigated.

In agreement with our work identifying a proapoptotic JAK/STAT5 pathway in CGNs, recent examination of the genetic targets of STAT5 demonstrates transcriptional regulation of prosurvival members of the Bcl-2 family. For example, STAT5 has been shown to negatively regulate the levels of Bcl-2 in osteosarcoma cells sensitized to undergo apoptosis (32). Similarly, both STAT5 isoforms were shown to bind to the promoter region of Bcl-x, a gene that is transcribed into prosurvival Bcl-xL and proapoptotic Bcl-extra short (Bcl-xS) (33, 43, 64). Therefore, it was of interest to determine whether Bcl-2 and/or Bcl-xL were transcriptional targets of STAT5 in CGNs subjected to Rac inhibition with ToxB. Our ChIP data show that STAT5 is recruited to the Bcl-xL promoter in ToxB-treated CGNs. These results suggest that STAT5 may transcriptionally repress Bcl-xL to tip the delicate balance between prosurvival and proapoptotic Bcl-2 proteins toward apoptosis. Consistent with this interpretation, we observed caspase-3 activation and classical apoptotic morphology subsequent to down-regulation of Bcl-xL protein levels. Although we show that STAT5 binding

## Rac Inhibition Induces STAT5-dependent Neuronal Apoptosis

to the promoter region of Bcl-xL increases in response to Rac inhibition, an alternative mechanism by which STAT5 may mediate transcriptional repression of Bcl-2 family proteins in the nucleus is through competitive binding to the transcriptional co-activator p300/cAMP-response element-binding protein (CREB)-binding protein (CBP) (65, 66). At the present time, we cannot exclude this as a possible mechanism of STAT5-dependent transcriptional repression of Bcl-xL during Rac inhibition.

Another potential mechanism by which STAT5 has been proposed to repress Bcl-xL transcription involves a cooperative interaction with the glucocorticoid receptor (GR). A recent report found that glucocorticoid treatment in lymphoid cells inhibited the transcription of Bcl-xL and decreased the ratio of Bcl-xL to the proapoptotic Bcl-xS in a STAT5B-dependent manner to induce apoptosis (13). Conversely, another report found that the GR can interact with STAT5 to up-regulate Bcl-xL as part of a prosurvival pathway activated by the GR agonist methylprednisolone in oligodendrocytes (67). Given the evidence suggesting that the GR can act in a cooperative manner with STAT5 to regulate the transcription of Bcl-xL, we sought to determine whether or not the GR was involved in STAT5A-mediated apoptotic signaling in CGNs subjected to ToxB treatment. In CGNs exposed to ToxB, the GR antagonist mifepristone provided no significant protection, indicating that the STAT5-dependent effects on Bcl-xL transcription are likely GR-independent in this cell system (data not shown).

In summary, we show that ToxB-induced inactivation of Rac GTPase results in the derepression of a novel proapoptotic JAK/STAT5 pathway. Although STAT1 was induced and STAT3 was phosphorylated following ToxB treatment, neither protein was responsible for inducing apoptosis of CGNs downstream of Rac inhibition. Rather, our data support a model in which ToxB-induced Rac inhibition in CGNs activates a novel proapoptotic JAK/STAT5 pathway that, following STAT5A phosphorylation and translocation to the nucleus, results in the transcriptional repression of prosurvival Bcl-xL and subsequent activation of caspase-3 and apoptosis. To our knowledge, our findings are novel in that they are the first to demonstrate a proapoptotic function for a JAK/STAT5 pathway in neurons.

## REFERENCES

- Olson, M. F., Ashworth, A., and Hall, A. (1995) An essential role for Rho, Rac, and Cdc42 GTPases in cell cycle progression through G1. *Science* **269**, 1270–1272
- Hill, C. S., Wynne, J., and Treisman, R. (1995) The Rho family GTPases RhoA, Rac1, and CDC42Hs regulate transcriptional activation by SRF. *Cell* **81**, 1159–1170
- Clark, E. A., King, W. G., Brugge, J. S., Symons, M., and Hynes, R. O. (1998) Integrin-mediated signals regulated by members of the rho family of GTPases. *J. Cell Biol.* **142**, 573–586
- Fukata, M., Kuroda, S., Nakagawa, M., Kawajiri, A., Itoh, N., Shoji, I., Matsuura, Y., Yonehara, S., Fujisawa, H., Kikuchi, A., and Kaibuchi, K. (1999) Cdc42 and Rac1 regulate the interaction of IQGAP1 with  $\beta$ -catenin. *J. Biol. Chem.* **274**, 26044–26050
- Tanaka, T., Tatsuno, I., Uchida, D., Moroo, I., Morio, H., Nakamura, S., Noguchi, Y., Yasuda, T., Kitagawa, M., Saito, Y., and Hirai, A. (2000) Geranylgeranyl-pyrophosphate, an isoprenoid of mevalonate cascade, is a critical compound for rat primary cultured cortical neurons to protect the cell death induced by 3-hydroxy-3-methylglutaryl-CoA reductase inhibi-
- tion. *J. Neurosci.* **20**, 2852–2859
- Linseman, D. A., Laessig, T., Meintzer, M. K., McClure, M., Barth, H., Aktories, K., and Heidenreich, K. A. (2001) An essential role for Rac/Cdc42 GTPases in cerebellar granule neuron survival. *J. Biol. Chem.* **276**, 39123–39131
- Jacquier, A., Buhler, E., Schäfer, M. K., Bohl, D., Blanchard, S., Beclin, C., and Haase, G. (2006) Alsin/Rac1 signaling controls survival and growth of spinal motoneurons. *Ann. Neurol.* **60**, 105–117
- Loucks, F. A., Le, S. S., Zimmermann, A. K., Ryan, K. R., Barth, H., Aktories, K., and Linseman, D. A. (2006) Rho family GTPase inhibition reveals opposing effects of mitogen-activated protein kinase kinase/extracellular signal-regulated kinase and Janus kinase/signal transducer and activator of transcription signaling cascades on neuronal survival. *J. Neurochem.* **97**, 957–967
- Igaz, P., Tóth, S., and Falus, A. (2001) Biological and clinical significance of the JAK-STAT pathway; lessons from knockout mice. *Inflamm. Res.* **50**, 435–441
- Yamauchi-Takahara, K., and Kishimoto, T. (2000) Cytokines and their receptors in cardiovascular diseases—role of gp130 signalling pathway in cardiac myocyte growth and maintenance. *Int. J. Exp. Pathol.* **81**, 1–16
- Watson, C. J., and Miller, W. R. (1995) Elevated levels of members of the STAT family of transcription factors in breast carcinoma nuclear extracts. *Br. J. Cancer* **71**, 840–844
- Kim, W. H., Hong, F., Radaeva, S., Jaruga, B., Fan, S., and Gao, B. (2003) STAT1 plays an essential role in LPS/D-galactosamine-induced liver apoptosis and injury. *Am. J. Physiol. Gastrointest. Liver Physiol.* **285**, G761–G768
- Rocha-Viegas, L., Vicent, G. P., Barañao, J. L., Beato, M., and Pecci, A. (2006) Glucocorticoids repress bcl-X expression in lymphoid cells by recruiting STAT5B to the P4 promoter. *J. Biol. Chem.* **281**, 33959–33970
- D'Mello, S. R., Galli, C., Ciotti, T., and Calissano, P. (1993) Induction of apoptosis in cerebellar granule neurons by low potassium: inhibition of death by insulin-like growth factor I and cAMP. *Proc. Natl. Acad. Sci. U.S.A.* **90**, 10989–10993
- Contestabile, A. (2002) Cerebellar granule cells as a model to study mechanisms of neuronal apoptosis or survival *in vivo* and *in vitro*. *Cerebellum* **1**, 41–55
- Vaudry, D., Falluel-Morel, A., Basille, M., Pamantung, T. F., Fontaine, M., Fournier, A., Vaudry, H., and Gonzalez, B. J. (2003) Pituitary adenylate cyclase-activating polypeptide prevents C2-ceramide-induced apoptosis of cerebellar granule cells. *J. Neurosci. Res.* **72**, 303–316
- Just, I., Selzer, J., Wilm, M., von Eichel-Streiber, C., Mann, M., and Aktories, K. (1995) Glucosylation of Rho proteins by *Clostridium difficile* toxin B. *Nature* **375**, 500–503
- Li, M., Linseman, D. A., Allen, M. P., Meintzer, M. K., Wang, X., Laessig, T., Wierman, M. E., and Heidenreich, K. A. (2001) Myocyte enhancer factor 2A and 2D undergo phosphorylation and caspase-mediated degradation during apoptosis of rat cerebellar granule neurons. *J. Neurosci.* **21**, 6544–6552
- Ahonen, T. J., Xie, J., LeBaron, M. J., Zhu, J., Nurmi, M., Alanen, K., Rui, H., and Nevalainen, M. T. (2003) Inhibition of transcription factor Stat5 induces cell death of human prostate cancer cells. *J. Biol. Chem.* **278**, 27287–27292
- Jank, T., and Aktories, K. (2008) Structure and mode of action of clostridial glucosylating toxins: the ABCD model. *Trends Microbiol.* **16**, 222–229
- Sahni, M., Raz, R., Coffin, J. D., Levy, D., and Basilico, C. (2001) STAT1 mediates the increased apoptosis and reduced chondrocyte proliferation in mice overexpressing FGF2. *Development* **128**, 2119–2129
- Stephanou, A., and Latchman, D. S. (2003) STAT-1: a novel regulator of apoptosis. *Int. J. Exp. Pathol.* **84**, 239–244
- Sironi, J. J., and Ouchi, T. (2004) STAT1-induced apoptosis is mediated by caspases 2, 3, and 7. *J. Biol. Chem.* **279**, 4066–4074
- Thomas, M., Finnegan, C. E., Rogers, K. M., Purcell, J. W., Trimble, A., Johnston, P. G., and Boland, M. P. (2004) STAT1: a modulator of chemotherapy-induced apoptosis. *Cancer Res.* **64**, 8357–8364
- Kaganoi, J., Watanabe, G., Okabe, M., Nagatani, S., Kawabe, A., Shimada, Y., Immura, M., and Sakai, Y. (2007) STAT1 activation-induced apoptosis of esophageal squamous cell carcinoma cells *in vivo*. *Ann. Surg. Oncol.*

- 14, 1405–1415
26. Soond, S. M., Carroll, C., Townsend, P. A., Sayan, E., Melino, G., Behrman, I., Knight, R. A., Latchman, D. S., and Stephanou, A. (2007) STAT1 regulates p73-mediated Bax gene expression. *FEBS Lett.* **581**, 1217–1226
  27. Takagi, Y., Harada, J., Chiarugi, A., and Moskowitz, M. A. (2002) STAT1 is activated in neurons after ischemia and contributes to ischemic brain injury. *J. Cereb. Blood Flow Metab.* **22**, 1311–1318
  28. Porter, A. G., and Jänicke, R. U. (1999) Emerging roles of caspase-3 in apoptosis. *Cell Death Differ.* **6**, 99–104
  29. Rawlings, J. S., Rosler, K. M., and Harrison, D. A. (2004) The JAK/STAT signaling pathway. *J. Cell Sci.* **117**, 1281–1283
  30. Wan, J., Fu, A. K., Ip, F. C., Ng, H. K., Hugon, J., Page, G., Wang, J. H., Lai, K. O., Wu, Z., and Ip, N. Y. (2010) Tyk2/STAT3 signaling mediates  $\beta$ -amyloid-induced neuronal cell death: implications in Alzheimer's disease. *J. Neurosci.* **30**, 6873–6881
  31. Blaskovich, M. A., Sun, J., Cantor, A., Turkson, J., Jove, R., and Sefti, S. M. (2003) Discovery of JSI-124 (cucurbitacin I), a selective Janus kinase/signal transducer and activator of transcription 3 signaling pathway inhibitor with potent antitumor activity against human and murine cancer cells in mice. *Cancer Res.* **63**, 1270–1279
  32. Chipoy, C., Brounais, B., Trichet, V., Battaglia, S., Berreut, M., Oliver, L., Juin, P., Rédini, F., Heymann, D., and Blanchard, F. (2007) Sensitization of osteosarcoma cells to apoptosis by oncostatin M depends on STAT5 and p53. *Oncogene* **26**, 6653–6664
  33. Nelson, E. A., Walker, S. R., Alvarez, J. V., and Frank, D. A. (2004) Isolation of unique STAT5 targets by chromatin immunoprecipitation-based gene identification. *J. Biol. Chem.* **279**, 54724–54730
  34. Chughtai, N., Schimchowitsch, S., Lebrun, J. J., and Ali, S. (2002) Prolactin induces SHP-2 association with Stat5, nuclear translocation, and binding to the  $\beta$ -casein gene promoter in mammary cells. *J. Biol. Chem.* **277**, 31107–31114
  35. Rigacci, S., Talini, D., and Berti, A. (2003) LMW-PTP associates and dephosphorylates STAT5 interacting with its C-terminal domain. *Biochem. Biophys. Res. Commun.* **312**, 360–366
  36. Faderl, S., Harris, D., Van, Q., Kantarjian, H. M., Talpaz, M., and Estrov, Z. (2003) Granulocyte-macrophage colony-stimulating factor (GM-CSF) induces antiapoptotic and proapoptotic signals in acute myeloid leukemia. *Blood* **102**, 630–637
  37. Rosen, R. L., Winestock, K. D., Chen, G., Liu, X., Hennighausen, L., and Finbloom, D. S. (1996) Granulocyte-macrophage colony-stimulating factor preferentially activates the 94-kD STAT5A and an 80-kD STAT5A isoform in human peripheral blood monocytes. *Blood* **88**, 1206–1214
  38. al-Shami, A., Bourgoin, S. G., and Naccache, P. H. (1997) Granulocyte-macrophage colony-stimulating factor-activated signaling pathways in human neutrophils. I. Tyrosine phosphorylation-dependent stimulation of phosphatidylinositol 3-kinase and inhibition by phorbol esters. *Blood* **89**, 1035–1044
  39. Storz, P., Döppeler, H., Pfizenmaier, K., and Müller, G. (1999) Insulin selectively activates STAT5b, but not STAT5a, via a JAK2-independent signalling pathway in Kym-1 rhabdomyosarcoma cells. *FEBS Lett.* **464**, 159–163
  40. Grimley, P. M., Dong, F., and Rui, H. (1999) Stat5a and Stat5b: fraternal twins of signal transduction and transcriptional activation. *Cytokine Growth Factor Rev.* **10**, 131–157
  41. Edamatsu, H., Gau, C. L., Nemoto, T., Guo, L., and Tamanoi, F. (2000) Cdk inhibitors, roscovitine and olomoucine, synergize with farnesyltransferase inhibitor (FTI) to induce efficient apoptosis of human cancer cell lines. *Oncogene* **19**, 3059–3068
  42. Wang, D., Stravopodis, D., Teglund, S., Kitazawa, J., and Ihle, J. N. (1996) Naturally occurring dominant negative variants of Stat5. *Mol. Cell. Biol.* **16**, 6141–6148
  43. Moucadel, V., and Constantinescu, S. N. (2005) Differential STAT5 signaling by ligand-dependent and constitutively active cytokine receptors. *J. Biol. Chem.* **280**, 13364–13373
  44. Korsmeyer, S. J., Shutter, J. R., Veis, D. J., Merry, D. E., and Oltvai, Z. N. (1993) Bcl-2/Bax: a rheostat that regulates an anti-oxidant pathway and cell death. *Semin. Cancer Biol.* **4**, 327–332
  45. Kobayashi, K., Takahashi, M., Matsushita, N., Miyazaki, J., Koike, M., Yaginuma, H., Osumi, N., Kaibuchi, K., and Kobayashi, K. (2004) Survival of developing motor neurons mediated by Rho GTPase signaling pathway through Rho-kinase. *J. Neurosci.* **24**, 3480–3488
  46. Kanekura, K., Hashimoto, Y., Kita, Y., Sasabe, J., Aiso, S., Nishimoto, I., and Matsuo, M. (2005) A Rac1/phosphatidylinositol 3-kinase/Akt3 anti-apoptotic pathway, triggered by AlsinLF, the product of the ALS2 gene, antagonizes Cu/Zn-superoxide dismutase (SOD1) mutant-induced motoneuronal cell death. *J. Biol. Chem.* **280**, 4532–4543
  47. Cheung, Z. H., Chin, W. H., Chen, Y., Ng, Y. P., and Ip, N. Y. (2007) Cdk5 is involved in BDNF-stimulated dendritic growth in hippocampal neurons. *PLoS Biol.* **5**, e63
  48. Mäkelä, J., Koivuniemi, R., Korhonen, L., and Lindholm, D. (2010) Interferon- $\gamma$  produced by microglia and the neuropeptide PACAP have opposite effects on the viability of neural progenitor cells. *PLoS One* **5**, e11091
  49. Colodner, K. J., and Feany, M. B. (2010) Glial fibrillary tangles and JAK/STAT-mediated glial and neuronal cell death in a *Drosophila* model of glial tauopathy. *J. Neurosci.* **30**, 16102–16113
  50. Giunta, B., Obregon, D., Hou, H., Zeng, J., Sun, N., Nikolic, V., Ehrhart, J., Shytle, D., Fernandez, F., and Tan, J. (2006) EGCG mitigates neurotoxicity mediated by HIV-1 proteins gp120 and Tat in the presence of IFN- $\gamma$ : role of JAK/STAT1 signaling and implications for HIV-associated dementia. *Brain Res.* **1123**, 216–225
  51. Dedoni, S., Olianas, M. C., and Onali, P. (2010) Interferon- $\beta$  induces apoptosis in human SH-SY5Y neuroblastoma cells through activation of JAK-STAT signaling and down-regulation of PI3K/Akt pathway. *J. Neurochem.* **115**, 1421–1433
  52. Granness, A., Poli, V., and Goppelt-Struebe, M. (2006) STAT3-independent inhibition of lysophosphatidic acid-mediated upregulation of connective tissue growth factor (CTGF) by cucurbitacin I. *Biochem. Pharmacol.* **72**, 32–41
  53. Byts, N., Samoylenko, A., Fasshauer, T., Ivanisevic, M., Hennighausen, L., Ehrenreich, H., and Sirén, A. L. (2008) Essential role for Stat5 in the neurotrophic but not in the neuroprotective effect of erythropoietin. *Cell Death Differ.* **15**, 783–792
  54. Mohapatra, S., Chu, B., Wei, S., Djeu, J., Epling-Burnette, P. K., Loughran, T., Jove, R., and Pledger, W. J. (2003) Roscovitine inhibits STAT5 activity and induces apoptosis in the human leukemia virus type 1-transformed cell line MT-2. *Cancer Res.* **63**, 8523–8530
  55. Um, M., and Lodish, H. F. (2006) Antiapoptotic effects of erythropoietin in differentiated neuroblastoma SH-SY5Y cells require activation of both the STAT5 and AKT signaling pathways. *J. Biol. Chem.* **281**, 5648–5656
  56. Choi, J. K., Kim, K. H., Park, H., Park, S. R., and Choi, B. H. (2011) Granulocyte macrophage-colony stimulating factor shows anti-apoptotic activity in neural progenitor cells via JAK/STAT5-Bcl-2 pathway. *Apoptosis* **16**, 127–134
  57. Bingisser, R. M., Tilbrook, P. A., Holt, P. G., and Kees, U. R. (1998) Macrophage-derived nitric oxide regulates T cell activation via reversible disruption of the Jak3/STAT5 signaling pathway. *J. Immunol.* **160**, 5729–5734
  58. Cavalcanti, E., Gigante, M., Mancini, V., Battaglia, M., Dittono, P., Capobianco, C., Cincione, R. I., Selvaggi, F. P., Herr, W., Storkus, W. J., Gesualdo, L., and Ranieri, E. (2010) JAK3/STAT5/6 pathway alterations are associated with immune deviation in CD8 T cells in renal cell carcinoma patients. *J. Biomed. Biotechnol.* **2010**, 935764
  59. Martín, P., Gómez, M., Lamana, A., Cruz-Adalia, A., Ramírez-Huesca, M., Ursúa, M. A., Yáñez-Mo, M., and Sánchez-Madrid, F. (2010) CD69 association with Jak3/Stat5 proteins regulates Th17 cell differentiation. *Mol. Cell Biol.* **30**, 4877–4889
  60. Krebs, D. L., and Hilton, D. J. (2001) SOCS proteins: negative regulators of cytokine signaling. *Stem Cells* **19**, 378–387
  61. Cooney, R. N. (2002) Suppressors of cytokine signaling (SOCS): inhibitors of the JAK/STAT pathway. *Shock* **17**, 83–90
  62. Terstegen, L., Gatsios, P., Bode, J. G., Schaper, F., Heinrich, P. C., and Graeve, L. (2000) The inhibition of interleukin-6-dependent STAT activation by mitogen-activated protein kinases depends on tyrosine 759 in the cytoplasmic tail of glycoprotein 130. *J. Biol. Chem.* **275**, 18810–18817

## Rac Inhibition Induces STAT5-dependent Neuronal Apoptosis

63. Borland, G., Bird, R. J., Palmer, T. M., and Yarwood, S. J. (2009) Activation of protein kinase C $\alpha$  by EPAC1 is required for the ERK- and CCAAT/enhancer-binding protein  $\beta$ -dependent induction of the SOCS-3 gene by cyclic AMP in COS1 cells. *J. Biol. Chem.* **284**, 17391–17403
64. Boise, L. H., González-García, M., Postema, C. E., Ding, L., Lindsten, T., Turka, L. A., Mao, X., Nuñez, G., and Thompson, C. B. (1993) bcl-x, a bcl-2-related gene that functions as a dominant regulator of apoptotic cell death. *Cell* **74**, 597–608
65. Zhu, M., John, S., Berg, M., and Leonard, W. J. (1999) Functional association of Nmi with Stat5 and Stat1 in IL-2- and IFN $\gamma$ -mediated signaling. *Cell* **96**, 121–130
66. Zhang, J., Yamada, O., Kawagishi, K., Araki, H., Yamaoka, S., Hattori, T., and Shimotohno, K. (2008) Human T-cell leukemia virus type 1 Tax modulates interferon- $\alpha$  signal transduction through competitive usage of the coactivator CBP/p300. *Virology* **379**, 306–313
67. Xu, J., Chen, S., Chen, H., Xiao, Q., Hsu, C. Y., Michael, D., and Bao, J. (2009) STAT5 mediates antiapoptotic effects of methylprednisolone on oligodendrocytes. *J. Neurosci.* **29**, 2022–2026